

# Strained condition parameters during brass backward extrusion with a high elongation coefficient

Shimov G.V.,<sup>1</sup>, Loginov Y.N.<sup>1,2</sup>, Bushueva N.I.<sup>1</sup>, Vorsin A.S.<sup>1,3</sup>

<sup>1</sup>Ural Federal University named after the first President of Russia B.N. Yeltsin, Mira street 19, Ekaterinburg, 620002, Russia

<sup>2</sup>M.N. Mikheev Institute of Metal Physics of the Ural Branch of the Russian Academy of Sciences

<sup>3</sup> ПАО «Каменск-Уральский завод по обработке цветных металлов»

Annotation. The brass backward extrusion boundary value problem with a elongation coefficient more than 700 is carried out. This process is consistent with production practices. The problem is solved using the DEFORM software module by the finite element method. The displacement velocities, strain rates and degree of strain are calculated. The difference between extrusion with moderate and high elongation coefficients is revealed. The moderate extraction coefficients during extrusion results to the formation of a deformation zone which boundaries which reach the container wall. The use of large extraction coefficients results to the deformation zone localization near the matrix extrusion die parallel land. The local level strain rates excess above the value  $1000 \text{ s}^{-1}$  is revealed.

## 1. Previous work

The two-phase brasses pressure shaping is an increased attention object, since in the presence of two phases due to an additional lever is created to control the properties of the material [1-3]. The two-phase brasses have a low ductility level in the hot state with rigid stress state schemes. They are usually processed not by rolling, but by extrusion. In this case, a high level of compression stresses increases the paste-forming properties. It is possible to obtain the product without destruction. An important question is whether the workpiece metal will be partially or completely in the temperature field corresponding to the high-temperature phase during hot deformation [4,5]. Related studies are aimed at the fixing possibility of this phase to improve the final product properties [6]. It is important whether the pressing is carried out in a direct or backward way [7]. The strain rate distribution and strain distribution during the deformation process is important. It is known that the distribution of these parameters is extremely heterogeneous from the two-phase brasses' extrusion. At the same time, the stress-strain properties level that the metal inherits depends on this distribution. The FEM for stress-strain state analyses is using by various software modules such as: DEFORM [8], QFORM [9] etc.

The work aim is to study the distribution of tensor and invariant characteristics of the stress-strain state by the finite-difference method in the single-channel backward extrusion of a rod made of two-phase brass.

### 1. 1. The calculation method description

The finite element method implemented in the DEFORM software module is used to analyze the extrusion scheme. The problem statement is carried out in 2D indication. Fig. 1, a shows a general view of the tools and the workpiece locations. Fig. 1, b shows an enlarged image of the area adjacent to the matrix extrusion die, with a finite elements mesh on the workpiece body. The tools and workpieces geometric parameters are represented by the following data: the container diameter  $D_k = 260 \text{ mm}$ , the ingot length  $L = 750 \text{ mm}$ , the ingot diameter  $D = 250 \text{ mm}$ ; the parallel land diameter and

length  $d_k = 9,8$  mm and 3,0 mm, respectively. Thus, the ratio  $L/D = 3$  is used. It is acceptable for the backward extrusion scheme since the friction effect on the container walls is leveled here. The elongation coefficient regarding to container in this case will be the value

$$\lambda = D_k^2/d_k^2 = 260^2/9,8^2 = 704, \quad (1)$$

accordingly, the strain degree

$$\varepsilon = \ln\lambda = 2*\ln(D_k/d_k) = 6,56. \quad (2)$$

The strain degree can also be estimated through the reduction rate over the area:

$$\varepsilon_0 = 100*(\lambda - 1) / \lambda = 99,85\%. \quad (3)$$

The latter value indicates that the very high deformations mode is realized in this case. A cylindrical coordinate system  $r\phi y$  is introduced during setting the problem. The following kinematic boundary conditions for axisymmetric deformation are used:

- for container wall:

$$V_r = 0; V_y = 0, \quad (4)$$

- for matrix extrusion die:

$$V_r = 0; V_y = 6 \text{ MM/c}. \quad (5)$$

The index "r" refers to the radial coordinate, the index "y" to the axial coordinate.

The problem scheme statement is shown in Fig. 1.

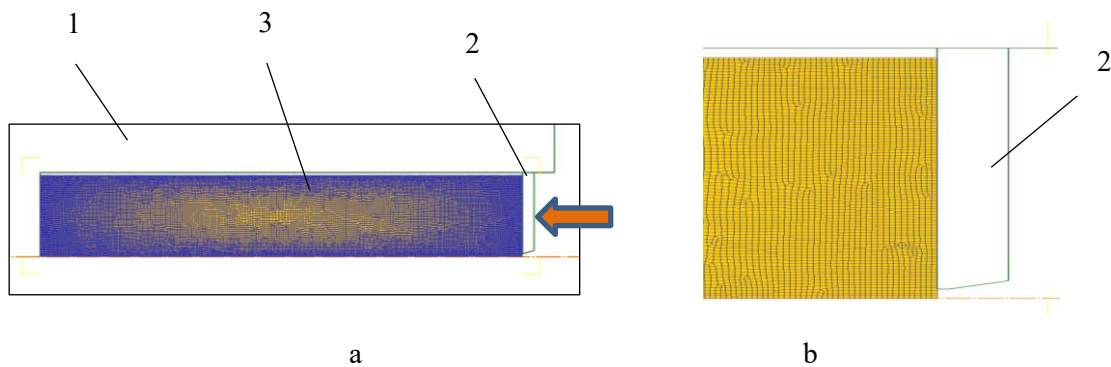


Fig. 1. The design process scheme (a) and an enlarged image of the metal part adjacent to the matrix extrusion die with the the finite element mesh display: 1-the wall of the container; 2-the matrix extrusion die; 3-the workpiece; the arrow shows the the matrix extrusion die movement direction

The statement is carried out with the finite elements number amount 26500. The setting conditions are as follows: the workpiece material in accordance with the standard DIN\_CuZn40Pb with properties in the temperature range 550...950 °C. The object type is plastic. The billet heating temperature consist 680 C°, the heating temperature of the container and matrix extrusion die consist 460 °C, matrix matrix extrusion die movement velocity – 6 mm/c (according to the production process data). The friction coefficient on the matrix extrusion die is 0.2. The heat transfer parameters are set according to the software module recommendations

## 2. Calculations results

Fig. 2, a shows the radial component distribution of the displacement velocity. It can be seen that the the symmetry condition process is satisfied: at the radial coordinate  $r = 0$ , the radial velocity  $V_r$  is zero. This velocity on the container wall surface is also consist zero due to the need to meet the condition that the deformable metal does not penetrate the tool. Figure 2, b shows the modulus of the displacement velocity vector distribution. The maximum value is close to 4000 mm/s. This value can also be calculated using the formula  $V_{\max} = V_y * \lambda = 6 * 703 = 4218$  mm/s.

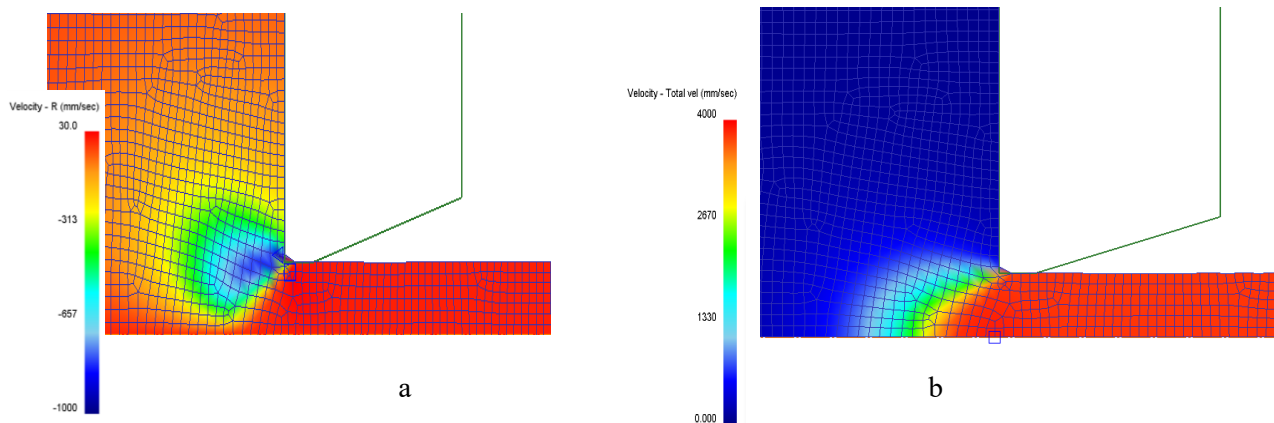


Figure 2. Display of the radial component of the displacement velocity (a) and the modulus of the displacement velocity vector (b), mm/s

The module of the displacement velocity vector has a maximum just on the extrusion axis in contrast to the radial component. (Fig. 2, b). This phenomenon is caused by the influence of large movements along this coordinate. In general, the field of displacement velocities does not extend to the entire the workpiece volume. It is localized near the matrix extrusion die mouth. This is the difference of extrusion with a large extraction coefficient.

The strain velocity tensor  $T_{\xi}$  characterizes strain of shortening or elongation, as well as shifts in individual volumes of the deformation zone in contrast to the displacement velocity vector. Fig. 3, a show the strain rate tensor  $\xi_{rr}$  component distribution. The highest values are reached near the matrix extrusion die parallel land. The component  $\xi_{rr}$  is no distribution to the extrusion axis centre in this case. Invariant value of the strain rate intensity  $\xi$  (fig. 3, b) essentially sets the deformation zone shape: this area can be bounded by a zone with radial curves. This area does not extend to the container wall. It is localized near the matrix extrusion die mouth in contrast to the case of extrusion with low and medium elongation coefficient. It should be noted that the strain rate intensity  $\xi$  obtained reaches the value  $1400 \text{ s}^{-1}$ . This is primarily due to the large values of deformation. Caution is aroused by the fact that the hardening curves graphs are not usually plotted for such high velocities. At best, the strain rate in material tests is limited to  $100 \text{ s}^{-1}$ . Therefore, the calculated data on the strain resistance are obtained by extrapolating the graphs for moderate velocity values. An important research area on the rheological materials properties would be to extend the range of strain rates to  $1000 \text{ s}^{-1}$ . This would improve the calculations performed accuracy.

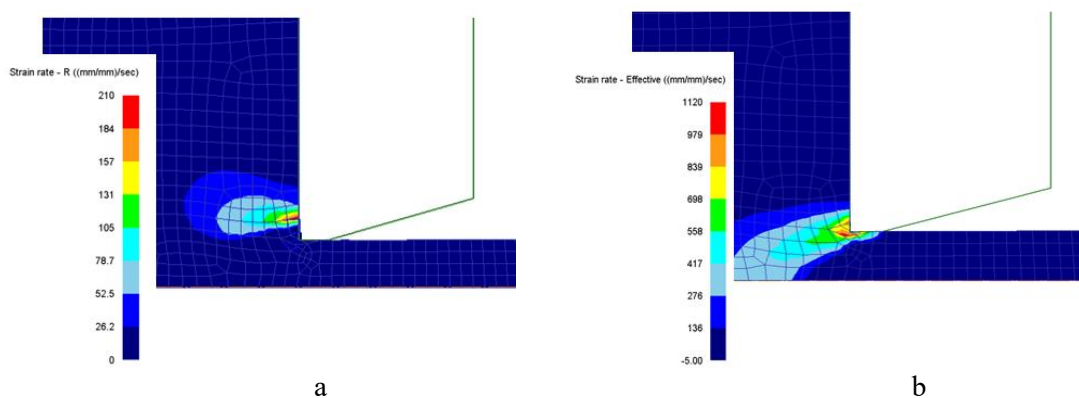


Рис. 3. Imaging the strain rate tensor component  $\xi_{rr}$  (a) and the strain rate intensity  $\xi$ ,  $\text{s}^{-1}$

### 3. The production process elements

The paper considers the real situation that occurs during the production of lead brass at the PJSC "Kamensk-Uralsky non-ferrous metal working plant". Figure 4, a shows a photo of the ingot loaded into the container and the matrix extrusion die attached to the movable die. Figure 4, b shows the coil view after extrusion.

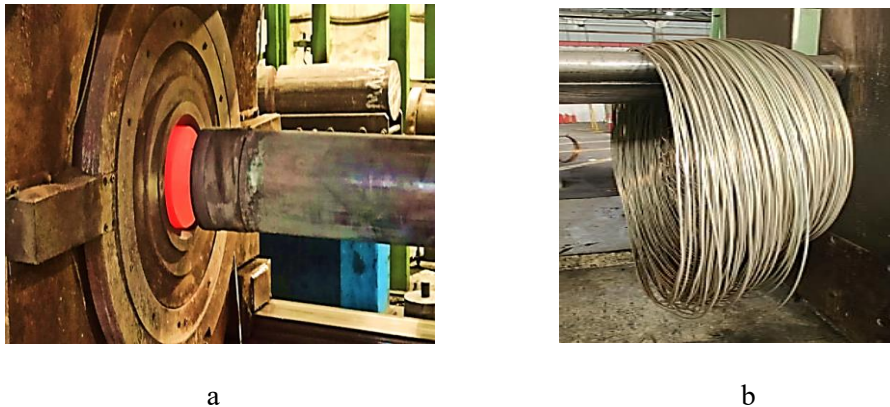


Рис. 4. Ingot and tool assembly during extrusion (a), finished product coil (b)

Conclusions. During the brass extrusion process with large elongation coefficients by the finite element method, it was revealed that the deformation zone does not reach the walls of the container. Deformations are localized near the matrix extrusion die mouth. It is established that the strain rates level exceeds the value of  $1000 \text{ s}^{-1}$ .

#### Ссылки

1. Fadhil, A.A., Ghattas, M.S., Iskander, B.A., Ajeel, S.A., Enab, T.A. Structural characterization and detecting processes of defects in leaded brass alloy used for gas valves production. *Alexandria Engineering Journal*. 2018. V. 57(3). P. 1301-1311
2. Illarionov, A.G., Loginov, Y.N., Stepanov, S.I., Illarionova, S.M., Radaev, P.S. Variation of the Structure-and-Phase Condition and Physical and Mechanical Properties of Cold-Deformed Leaded Brass Under Heating 2019 *Metal Science and Heat Treatment* 61(3-4), c. 243-248
3. Dhinwal, S.S., Shukla, A.J., Biswas, S., Chouhan, D.K. Evolution of microstructure and crystallographic texture in  $\alpha$ - $\beta$  Brass during equal channel angular pressing. *Materials Characterization* 2020. V. 163. No.110270.
4. Pugacheva, N.B., Pankratov, A.A., Frolova, N.Yu., Kotlyarov, I.V. Structural and phase transformations in  $\alpha + \beta$  brasses 2006 *Russian Metallurgy (Metally)* 2006(3), c. 239-248.
5. Loginov, Y.N., Ovchinnikov, A.S. Increase in the Uniformity of Structure and Properties of Extruded Workpieces of Alpha + Beta Lead Brasses. 2015 *Metallurgist* 59(3-4), c. 342-347
6. Momeni, A., Ebrahimi, G.R., Faridi, H.R. Effect of chemical composition and processing variables on the hot flow behavior of leaded brass alloys. 2015. *Materials Science and Engineering A*. V. 626, P. 1-8.
7. Chang, C.-C., Hsu, C.-H., Lai, J.-C. Effects of grain size and lubricating conditions on micro forward and backward hollow extrusion of brass. 2014. *Applied Mechanics and Materials*. 479-480, P. 8-12.

8. Kargin, V.R., Deryabin, A.Y. Simulation of the Final Stage of the Direct Extrusion Method of Large-Size Rods at Small Elongations. 2018 Russian Journal of Non-Ferrous Metals. 59(6), P. 632-636.
9. Ershov, A.A., Kotov, V.V., Loginov, Yu.N. Capabilities of QForm-extrusion based on an example of the extrusion of complex shapes. 2012 Metallurgist 55(9-10), c. 695-701.